Journal of Applied Polymer Science

Permeability of small molecules through vapor deposited polymer membranes

Ali Tufani,[1] Gozde Ozaydin Ince[1,2]

[1]Materials Science and Nanoengineering Program, Faculty of Engineering and Natural Sciences, Sabanci University, 34956 Istanbul, Turkey

[2]Sabanci University Nanotechnology Research and Application Center, 34956 Istanbul, Turkey

Correspondence to: G. O. Ince (E-mail: gozdeince@sabanciuniv.edu)

ABSTRACT: Free-standing, thin films of poly(2-hydroxyethyl methacrylate), p(HEMA), membranes deposited by initiated chemical vapor deposition (iCVD) technique are presented. Systematic studies of permeation of model dye molecules through these free-standing thin films are performed and effects of process parameters on the permeability and selectivity of the membranes synthesized using an all-dry process are demonstrated for the first time. Permeation studies of model dye molecules show that the diffusion of large dye molecules through the membrane is faster than the smaller dye molecules, due to loss of conformation entropy. Mesh sizes of the membranes are controlled by tuning the crosslink ratio of the polymer and diffusion coefficients of alizarin yellow model dye molecules are obtained as 0.44×10^{-7} and 1.71×10^{-7} cm^2/s for high and low crosslinked membranes, respectively. Selectivity of the membranes is also demonstrated by the permeation studies of dyes with similar sizes but different polarities and the permeability coefficient of the hydrophilic dye is observed to be 30 times larger than that of the hydrophobic dye of similar size. © 2015 Wiley Periodicals, Inc. J. Appl. Polym. Sci. **2015**, *132*, 42453.

KEYWORDS: hydrophilic polymers; membranes; radical polymerization

Received 28 February 2015; accepted 4 May 2015

DOI: 10.1002/app.42453

INTRODUCTION

Polymeric membranes with their biocompatible nature and application-tailored physical characteristics find uses in a wide variety of applications, including drug delivery devices, artificial organs, or separation and purification systems.[1,2] Many of these applications require selective passage of molecules between two different media separated by a membrane. The flow of molecules through the membrane can be regulated by tuning the membrane properties according to the size, charge, or functionalities of permeate molecules.[3] The thickness of the separating membrane generally needs to be minimized to improve the permeation time and flux. These constraints on the membrane properties necessitate utilization of membrane synthesis techniques, which allow separate control of the chemical composition and physical dimensions of the membranes.

Interfacial polymerization,[4] electrospinning,[5] layer-by-layer (LbL) deposition,[6] and molecular imprinting[7] are few of the widely used techniques to synthesize free-standing polymer membranes with well defined chemical composition. However, challenges of fabricating ultra-thin membranes or use of hazardous solvents are major drawbacks of these techniques. Deposition of highly crosslinked polymers is also a challenge, as the conventional techniques generally require dissolving the polymers in solvents.

Recent advances in the processing techniques increased the interest in membranes synthesized from functional polymers.[8] The response of the polymer to external stimuli by undergoing physical changes can be used to control the permeation dynamics in the membrane.[9,10] For example, hydrogels are widely used in controlled release applications where the release can be triggered by stimuli and the release kinetics can be controlled by tuning the chemical and physical properties of the polymer matrix.[11] Poly(2-hydroxyethyl methacrylate) is one of the most widely used polymers in release applications due to its biocompatible nature, tunable mesh size to control swelling and high mechanical strength.[12,13]

An important property that regulates the diffusion of the molecules through the polymer membrane is the swelling ratio of the polymer.[14] For improved diffusion rates the polymer mesh size in the solvated state should be comparable to the permeate size whereas in the collapsed state the mesh size should preferably be smaller to inhibit diffusion for a better control of the

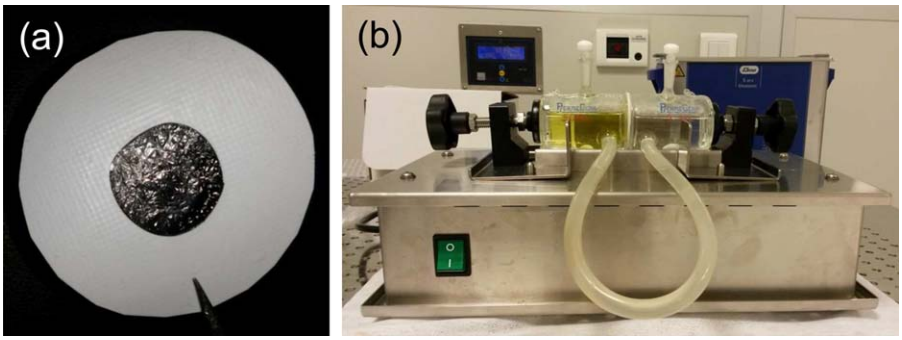

Figure 1. (a) Free-standing p(HEMA) membrane and the white plastic frame surrounding it are shown. (b) Side-bi-side diffusion cell used for permeation tests is shown. [Color figure can be viewed in the online issue, which is available at www.interscience.wiley.com.]

release mechanism. This requires tuning of the polymer mesh size in accordance with the permeate size by varying the crosslink density of the hydrogel.

Integration of responsive polymers in membranes requires the functional groups of the polymers to remain intact during synthesis. Furthermore, due to inverse relation between the membrane thickness and molecular flux through membrane, ultra thin membranes should be synthesized for improved permeability. In this study, iCVD is used to synthesize ultra thin, free-standing membranes of p(HEMA) polymer, which is highly swellable. iCVD is an all-dry, solventless polymer deposition technique, which allows coating of delicate substrates with functional polymers.[15] The radical molecules that are activated by the heated filaments in the vacuum chamber react with the vinyl bonds of the monomer molecules adsorbed on the surface, initiating the polymerization reaction. As the polymerization occurs on the substrate surface the chemical composition of the deposited polymer can be tuned real-time. The vapor phase precursors allow the control of film thickness in the nm level. Ultra thin functional polymers with fine-tuned responses can therefore be fabricated using iCVD.[16]

The study presented here aims to develop and characterize nonporous, free-standing thin film membranes of functional p(HEMA) polymers with tunable mesh size to control the diffusion of model dye molecules. Although studies on p(HEMA) deposition using iCVD exist in literature,[17] studies on the ultra-thin free-standing p(HEMA) membranes and their permeability properties are very few. In bioapplications, such as artificial organs or transdermal drug delivery, the permeability and selectivity of the separating membranes are the critical factors affecting the performance, thereby making the studies involving improvements of membrane properties quite important. Differences between the mechanical properties of the free-standing polymer membranes and the back-supported thin films or bulk polymers necessitate separate studies on free-standing membranes. However, due to the difficulties in synthesizing free-standing polymer thin films with different mesh sizes using conventional fabrication techniques, reports on the permeability properties of free-standing polymers are limited. In this paper, a systematic study on fabrication of p(HEMA) membranes with different mesh sizes is presented. The mesh size of the membranes is controlled by tuning the deposition parameters and the effects of dye size and polarity on the permeation rate are investigated.

MATERIALS AND METHODS

Membrane Preparation

Free-standing polymer thin film membranes were prepared by depositing the polymer thin film on a sacrificial layer using iCVD and subsequently removing the sacrificial layer. The sacrificial layer was prepared by spin coating of Polyacrylic Acid (PAA) solution (2.5 g PAA and 7.5 g water) on a Si wafer at 1500 rpm for 15 s followed by baking spin coated solution for 2−3 min on a hot plate at 80−100°C.

P(HEMA) thin films with 1000 ± 10 nm thickness were then coated on the sacrificial layer using iCVD. Details of fabrication of free-standing films via iCVD are given elsewhere.[18] The monomer HEMA, the cross-linking EGDMA, the initiator TBPO were used as received, without further purification. HEMA and EGDMA were vaporized in the jars at 70°C and 80°C, respectively and TBPO was at room temperature. The vapors were then delivered to the vacuum chamber from different ports. The flowrates of N_2 and TBPO were fixed at 1 sccm while the flowrates of the monomers were varied between 0.05 and 0.5 sccm to obtain polymers with different crosslink ratios. The operating pressure was set to 250 mTorr and the filament and stage temperatures were kept at 270°C and 30°C, respectively during the depositions. The thickness of the samples was monitored real-time using a laser interferometry system and the deposition was stopped at a film thickness of 1000 nm.

After the iCVD process, a plastic holder of 5 cm diameter with a 2 cm diameter hole at the center was glued on the polymer layer surface [Figure 1(a)] and then the sample was immersed in DI water to dissolve the PAA layer. The p(HEMA) layer was detached from the Si substrate following the removal of PAA layer.

Polymer Coating Characterization

Fourier transform infrared (FT-IR) (Thermo-Nicolet iS10 FTIR) measurements were performed in normal transmission mode. Spectra were acquired over the range of 400−4000 cm^{-1} with a 4 cm^{-1} resolution for 64 scans. All spectra were baseline-corrected and normalized to a thickness of 1000 nm.

Accurate measurements of film thickness were performed using a spectroscopic ellipsometer (M2000 Spectroscopic Ellipsometer J. A.Wollam Co., Inc.). All thickness measurements were made at 65, 70, and 75 incidence angle using wavelengths ranging from 315 to 718 nm. The Cauchy model was used to fit data.

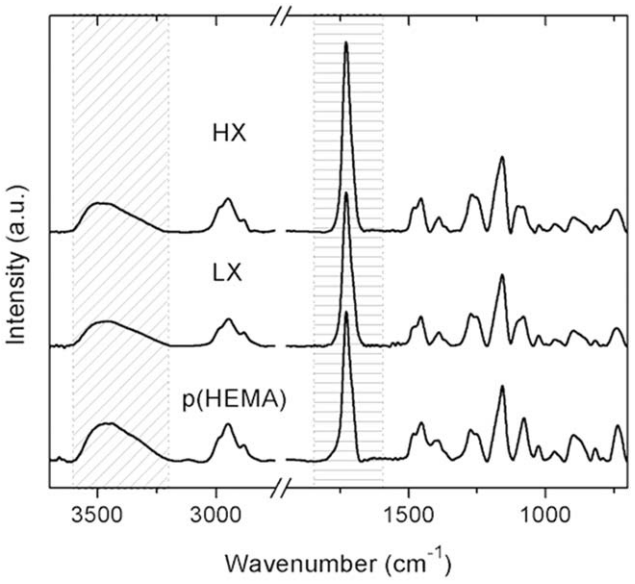

Figure 2. FTIR spectra of the deposited uncrosslinked, high crosslinked (HX) and low crosslinked (LX) p(HEMA) membranes. The peaks representing the C═O stretching vibrational modes are shaded with horizontal lines, while the peaks respresenting the O—H vibrational modes are shaded with diagonal lines.

The swelling ratios of the polymer films were measured in a heated liquid cell with nominal angle of incidence of 75 degrees. The change in thickness of the films as water was introduced, was recorded as a function of time. The swelling ratio was then calculated by t_0/t, where t_0 and t are the thicknesses of the dry and swollen polymers, respectively. The swelling experiments were repeated multiple times and the samples were dried after each experiment.

The elastic moduli of the films were measured using the peak force quantitative nanomechanics (QNM) mode of the Multi-Mode AFM. First, force curves on the polymer surface were obtained at different locations and then, Hertzian fit modeling was applied to these force-versus-separation curves.

Permeation Experiments

Permeation studies of dye molecules through the polymer membranes were performed in a side-by-side diffusion cell (50 mL PermeGear Side-bi-Side Diffusion Cell) with an effective membrane area, A, of 3.14 cm^2 at atmospheric pressure [Figure 1(b)]. The free-standing polymer membrane was placed between two cylindrical glass chambers of 50 mL volume. One chamber was filled with feed solution and the other chamber was filled with DI water, solutions in both chambers were stirred continuously by magnets throughout the experiments. The experiments were performed at 25°C and 50°C. The feed solutions were prepared at different dye concentrations. The model dyes used for the experiments were Phloroglucinol (Phl), Alizarin Yellow (AY) and 4-Phenylazodiphenylamine (PADPA). Three different dye solutions were used in the experiments: Phl (0.6 g/L), AY (0.07 g/L) and AY + PADPA (0.07 g/L –each). Permeation rate of the dye molecules were calculated by measuring the dye concentration on the permeate side periodically. This was done by taking 3.5 mL of the permeate solution and performing UV-Vis measurements (Shimadzu UV-3150). After the measurements the solution was poured back into the permeate chamber.

To find the solute partition coefficient, K, which was used to calculate the diffusion coefficient, the membranes were immersed in dye solution for 7 days and the ratio of the dye concentration in the membrane to the concentration in the solution was calculated.

RESULTS AND DISCUSSION

The thickness-normalized and baseline-corrected FTIR spectra of the p(HEMA) thin films with different crosslink ratios are shown in Figure 2. The peaks observed at 3550−3050 cm^{-1} and 1750−1690 cm^{-1} correspond to the vibrational modes of O—H stretching and C═O stretching respectively. Intensity of the O—H stretching peak decreases with respect to C═O stretching peak as the EGDMA ratio in the feed is increased, confirming an increase in the crosslink ratio. The crosslink percentages of the deposited films are calculated using the FTIR spectra where the areas under the peaks are proportional to the concentrations of C═O or O—H groups in the films, assuming similar bond oscillator strengths for both HEMA and EGDMA.[17] The ratio of EGDMA to HEMA in the film, which is related to the crosslink ratio, can be found using:

$$\frac{EGDMA}{HEMA} = \frac{(A_{C=O} - rA_{O-H})/2}{rA_{O-H}} \quad (1)$$

where A represents the area under the peak of the corresponding vibrational mode in the copolymer films and r is the ratio of $A_{C=O}$ to A_{O-H} in the linear p(HEMA) film. Table I shows the crosslink ratios of the deposited p(HEMA) films.

The reactivity ratios of the monomer precursors are used to determine the chemical composition of the copolymer films. The reactivity ratios are calculated using the Fineman-Ross copolymer equation modified to account for the two vinyl groups of the EGDMA monomer, which is given by:[19]

$$\frac{f'_{EGDMA}(1-2F_{EGDMA})}{F_{EGDMA}(1-f'_{EGDMA})} = r_{HEMA} + \left[\frac{f'^2_{EGDMA}(F_{EGDMA}-1)}{F_{EGDMA}(1-f'_{EGDMA})^2}\right] r_{EGDMA} \quad (2)$$

In iCVD, polymerization mechanism takes place on the surface, therefore the rate of polymerization depends on the surface monomer concentration f', instead of gas monomer concentration f_{EGDMA} which is generally used in the Fineman-Ross relation. In eq. (2), f'_{EGDMA} and F_{EGDMA} correspond to the surface mole fraction of EGDMA monomer and the mole fraction of

Table I. Deposition Parameters and the Crosslink Ratios of the iCVD Deposited p(HEMA) Free-Standing Films

	Flow rate (sccm)		P_m/P_{sat}		
Samples	HEMA	EGDMA	HEMA	EGDMA	Crosslink ratio
LX	0.5	0.086	0.182	0.404	0.32
HX	0.5	0.14	0.179	0.646	0.47

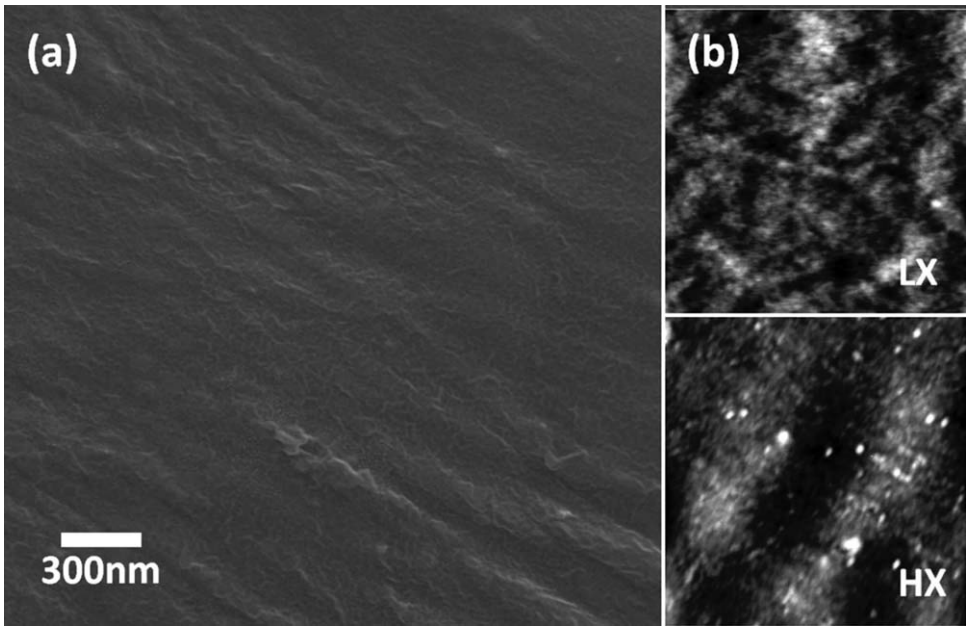

Figure 3. (a) SEM image of the free-standing HX p(HEMA) membranes before the diffusion tests. (b) AFM surface images (1 μm × 1 μm) of the LX and HX p(HEMA) membranes before the diffusion tests. The RMS roughness of the samples is less than 5 nm.

the EGDMA in the polymer, respectively, whereas r_{EGDMA} and r_{HEMA} correspond to the reactivity ratios of the monomers. The mole fraction of the EGDMA is determined from the FTIR analysis as described in the previous section. In Henry's law limit for low surface concentrations, the BET isotherm predicts linear relation between the amount of monomer on the surface and the P_m/P_{sat} values, where P_m is the partial and P_{sat} is the saturation pressures of the monomer.[20] Thus partial and saturation pressures of the monomers can be used to obtain the f'_{EGDMA} and f'_{HEMA} values. Using eq. (2), the reactivity ratios of EGDMA and HEMA are found as 0.169 and 0.886 respectively, confirming copolymerization.

Figure 3(a) shows the SEM image of a free-standing membrane. The AFM surface images of the low (LX) and high crosslinked (HX) polymer films show that the films are uniform with no phase segregation and the surface roughness is below 5 nm [Figure 3(b)]. Furthermore, the elastic moduli of the membranes are measured as 28.64 MPa for high crosslinked and 21.67 MPa for low crosslinked films by using the QNM mode of the AFM. If the membranes are carefully handled avoiding cracks, the membranes can be reused in the permeation studies, confirming their stability.

The permeation of the molecules through the membrane depends on the relative sizes of the molecules to that of the mesh size of the polymer. Therefore, tuning the mesh size of the polymer via adjusting the crosslink ratio enables control of the permeation mechanism. The average molecular weight, $\bar{M}_C$, between crosslinks, which is related to the mesh size, ξ, can be calculated using:[21]

$$\frac{1}{\bar{M}_C}=\frac{1}{\bar{M}_n}-\frac{\frac{\bar{v}}{V}\left[\ln(1-\upsilon_s)+\upsilon_s+\chi(\upsilon_s)^2\right]\left[1-\frac{M_r}{2\bar{M}_C}(\upsilon_s)^{2/3}\right]^3}{\left[(\upsilon_s)^{1/3}-\frac{1}{2}\upsilon_s\right]\left[1+\frac{M_r}{2\bar{M}_C}(\upsilon_s)^{1/3}\right]^2} \quad (3)$$

where $\bar{M}_n$ is the number average molecular weight which is large enough so that the first term on the right hand side can be neglected.[22] V is the molar volume of water (18 cm^3/mol), M_r is the molecular weight of the HEMA repeat unit (130 g/mol) and $\bar{v}$ is the specific volume of p(HEMA) (0.87 cm^3/g). χ is the Flory-Huggins interaction parameter and is taken as 0.681 in this study for p(HEMA) polymers crosslinked with EGDMA.[23] The ratios of the dry to wet thickness of the polymers, denoted as υ_s, are obtained from ellipsometry measurements performed on polymer films deposited on Si substrates and they are 0.69 and 0.75 for low and high crosslinked samples, respectively. Repeating the swelling tests multiple times confirms that the swelling of the films are reversible.

Reports on the effects of substrate confinement on the swelling of the polymer films exist in literature, reporting less swelling observed in surface-attached polymer films compared to that of nonattached films.[24] Furthermore, reports on the spin-coated films show that surface confinement effects on the swelling ratio are negligible for the nonattached ultra-thin films.[25] In the study presented here the polymer films are directly deposited and physisorbed on the substrate without any surface attachments, which would effect the polymer chain mobilization. The values of $\bar{M}_c$ for low and high crosslinked samples are determined as 152.43 g/mol and 127.34 g/mol, using eq. (3).

The mesh size of the deposited polymers, ξ, can be determined using the relation:

$$\xi=(\upsilon_s)^{-1/3}l\left(\frac{2\bar{M}_C}{M_r}\right)^{1/2}C_n^{1/2} \quad (4)$$

where C_n is the characteristic ratio for HEMA, which is taken as 6.9,[26] and l is the C—C bond length, which is 0.154 nm. The

mesh sizes of the low and high crosslinked samples are, then, calculated as 0.651 nm and 0.575 nm, respectively. The larger mesh size observed at low EGDMA content is due to low crosslinking of the films confirming that the mesh size can be controlled by tuning the chemical composition. P(HEMA-*co*-EGDMA) films with mesh sizes ranging from 0.34 to 0.75 nm can be obtained using the system parameters covered in this study and the synthesized films show no phase segregation as confirmed by AFM surface analysis. Yague *et al.*[27] observed mesh sizes ranging from 0.45 nm to 2.0 nm as HEMA/EGDA ratio increased from 0.45 to 1. As the HEMA content in the films increased, dissolution of the polymer films was observed. The dissolution of the uncrosslinked pHEMA films can be attributed to the low molecular weight of the deposited films. Dissolution of the uncrosslinked pHEMA films is not observed at ultrahigh molecular weights of 820,000 g/mol due to the entanglement of the long polymer chains.[28] The molecular weight of the deposited films, on the other hand, can be controlled by changing the ratio of initiator/monomer flowrates. Initiator to monomer flowrate ratios of 20, as used in our study, give short- chained, low M_w polymers, compared with ultrahigh M_w polymers obtained at initiator to monomer flowrate ratios of 0.5.[28]

Tuning of the mesh size is critical for membrane applications that rely on size exclusion. In the study reported here, the size selection characteristics of the membranes are studied using hydrophilic model dyes and the permeation through the free-standing polymer films with different mesh sizes are monitored using a diffusion cell. As the model dyes, hydrophilic alizarin yellow molecules and larger phloroglucinol molecules and relatively hydrophobic 4-Phenylazodiphenylamine molecules are used.

The change in dye concentration as a function of time on the receptor end is recorded and the solute permeability coefficient, *P*, is determined using:

$$Ln\left(1-\frac{2c[t]}{c[0]}\right)=-\left(\frac{2AP}{V}\right)t \quad (5)$$

where $c[0]$ is the initial dye concentration in the donor cell, $c[t]$ is the concentration at time t in the receptor cell, V is the cell volume (50 mL) and A is the effective membrane area (3.14 cm^2).

Figure 4 shows the change in dye concentration in the receptor cell as a function of time for low and high crosslinked samples. The permeability coefficient, *P*, can be determined from the slope using eq. (5) for each dye tested with membranes of different mesh sizes.

The solute diffusion coefficient, *D*, can then be calculated using:

$$D=\frac{P\delta}{K} \quad (6)$$

where δ is equilibrium membrane thickness (as obtained from the swelling cell ellipsometer experiments) and K is the partition coefficient. The equilibrium thickness values are measured as 1660 ± 20 nm and 1820 ± 10 nm, for high and low crosslinked membranes. K values are obtained as 0.048 and 0.041 for AY and Phl, respectively. Table II shows the P and D values obtained for different dyes and mesh sizes.

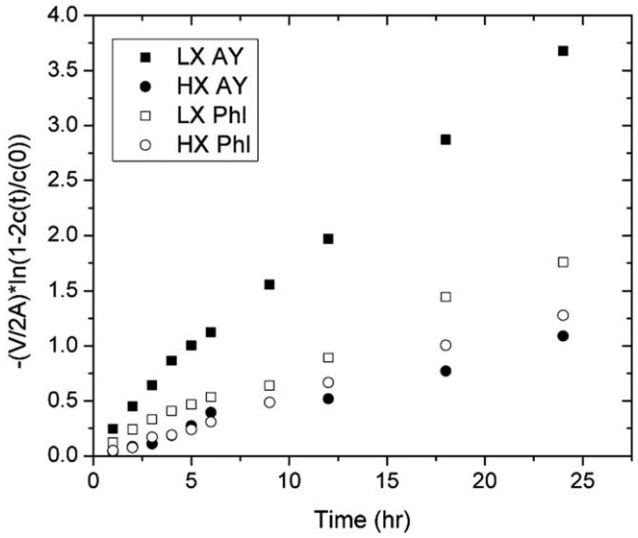

Figure 4. Plot of eq. (5) where $y(t) = -(V/A)*\ln(1-c(t)/c(0))$ showing the change in dye concentration as a function of time for low and high crosslinked samples tested with AY and Phl dyes. The slopes of the plots give the permeability coefficient, *P*.

Critical dye dimensions that affect the permeation of the dye molecules through the polymer are the solvent excluded diameter and the total polar surface area. The former is related to size exclusion as the relative diameter compared to mesh size of the polymer affects diffusion of the dye. On the other hand, total polar surface area, which is the sum of surface areas of all polar groups, is related to the hydrophilicity of the polymer; larger surface area indicating increased hydrophilicity. Solvent excluded sizes of AY and Phl are reported as 197.179 $Å^3$ and 90.42 $Å^3$, and total polar surface areas are 134.06 $Å^2$ and 60.69 $Å^2$, respectively.[29] Comparing the values, AY molecules are larger and more hydrophilic than Phl molecules.

The mesh size of the polymer is another factor that affects the permeation of the dye. As the mesh size increases the dye molecules can easily diffuse through the membrane due to increased free volume, therefore higher permeation rates are observed. Under the same conditions, both AY and Phl dyes have larger permeability and diffusion coefficients in low crosslinked (LX) polymer membranes compared to that of the highly crosslinked (HX) membranes, with smaller mesh size.

For the LX membranes with large mesh size, permeation coefficient of the larger dye AY is higher than that of the smaller dye Phl. Although polarity is also effective in improving the permeation of AY dyes in hydrophilic polymer, the main factor is the interplay between different entropies. While the entropy of mixing favors the smaller dyes to diffuse inside the pores of the polymer, the loss of conformation entropy leads to faster diffusion of larger dye molecules through the polymer mesh. Therefore, the higher permeation and diffusion coefficients of AY compared to that of Phl molecules in the LX membranes can be explained by loss of conformation entropy favoring faster diffusion of AY molecules through the p(HEMA) mesh.

Table II. Permeability and Diffusion Coefficients of Model Dyes Tested on Membranes with Different Mesh Sizes

Sample	Mesh size (nm)	Dye	Temperature (°C)	Permeability coefficient ($\times 10^{-5}$ cm/s)	Difffusion coefficient ($\times 10^{-7}$ cm^2/s)
HX	0.575	Phl	25	1.5	0.61
LX	0.651	Phl	25	3.13	0.95
HX	0.575	AY	25	1.27	0.44
LX	0.651	AY	25	4.48	1.71
LX	0.651	AY	50	8.3	3.16
LX	0.651	AY	25	1.25	0.24
		4PAP		0.30	0.008

On the other hand, for the HX membranes, AY had slightly lower permeation coefficient compared to Phl. This can be attributed to the smaller mesh sizes of the HX membranes. For dyes that are larger than the mesh size, size exclusion principle applies and the polymer acts as a molecular sieve, permitting only smaller dyes. For the two dyes studied here, the size of the larger dye AY is comparable to the mesh size of the highly crosslinked polymer membrane, leading to significantly reduced permeation of AY, compared to Phl which is smaller than the mesh size.

The effect of temperature on the diffusion rate of the AY dye is studied by repeating the same experiments at different temperatures. An increase in temperature of 25°C, increased the diffusion coefficient in accordance with $D \propto \exp(-\frac{1}{RT})$.[30]

The selectivity of the membranes with respect to permeant polarity is tested using AY and 4-Phenylazodiphenylamine (PADPA), which is similar to AY in size but significantly more hydrophobic, lacking the -OH and -NO_2 groups of AY. The feed solution used in the permeation studies, contains both dyes with same concentrations. Figure 5 shows the individual permeation rates of AY and PADPA dyes through LX membranes. Although both dyes are permeable, faster permeation of AY molecules can be attributed to the polarity of the hydrophilic AY molecules. The selective nature of the hydrophilic membranes is also confirmed by permeation coefficient of AY that is observed to be approximately 30 times larger than that of PADPA as shown in Table II. The selectivity of the membranes with respect to polarity can further be improved by adding polar functionalities to the polymer, which increase interaction with the polar dye molecules.

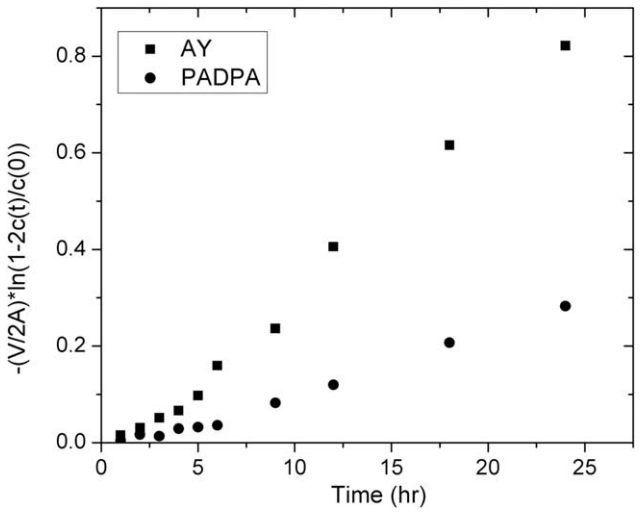

Figure 5. Plot of eq. (5) as a function of time showing the selectivity of the LX membranes tested with AY and PADPA dyes simultaneously.

CONCLUSIONS

In summary, we have demonstrated that, free-standing thin film polymer membranes can be fabricated using iCVD, an all-dry vapor phase polymer deposition technique. The mesh size of the deposited polymer membranes could be tuned by changing the crosslink ratio of the polymers. Tuning the mesh size allowed to control the permeation of small molecules with different size and polarities and via systematic diffusion studies, permeation and diffusion coefficients of the molecules were obtained. Difference in polarities of the permeants enabled selective permeation of the small molecules through the membranes. Due to the ability to control the chemical composition and mesh size, the membranes fabricated via iCVD technique may find applications in areas ranging from chromatography to molecular separation.

ACKNOWLEDGMENTS

This work was supported by the TUBITAK (The Scientific and Technological Research Council of Turkey) Career Development Program (Grant 112M315) and TUBA (Turkish Academy of Sciences) Young Scientist Award Program.

REFERENCES

1. Stamatialis, D. F.; Papenburg, B. J.; Gironés, M.; Saiful, S.; Bettahalli, S. N. M.; Schmitmeier, S.; Wessling, M. *J. Membr. Sci.* **2008**, 308(1–2), 1.
2. Geise, G. M.; Seung Lee, H.-S.; Miller, D. J.; Freeman, B. D.; McGrath, J. E.; Paul, D. R. *J. Polym. Sci. Part B: Polym. Phys.* **2010**, *48*, 1685.
3. Baker, R. W. Membrane Technology and Applications, 2nd ed.; Wiley: New York, NY, **2004**.
4. Song, Y.; Sun, P.; Henry, L. L.; Sun, B. *J. Membr. Sci.* **2005**, *251* (1–2), 67.

5. Wang, R.; Liu, Y.; Li, B.; Hsiao, B. S.; Chu, B. *J. Membr. Sci.* **2012**, *392*, 167.
6. Farhat, T. R.; Hammond, P. T. *Adv. Funct. Mater.* **2005**, *15*, 945.
7. Ulbricht, M. *J. Chromatography B* **2004**, *804*, 113.
8. Ulbricht, M. *Polymer* **2006**, *47*, 2217.
9. Tokarev, I.; Minko, S. *Adv. Mater.* **2009**, *21*, 241.
10. Wandera, D.; Wickramasinghe, S. R.; Husson, S. M. *J. Membr. Sci.* **2010**, *357*(1-2), 6.
11. Tokarev, I.; Minko, S. *Adv. Mater.* **2010**, *22*, 3446.
12. Weaver, J. V. M.; Bannister, I.; Robinson, K. L.; Bories-Azeau, X.; Armes, S. P.; Smallridge, M.; McKenna, P. *Macromolecules* **2004**, *37*, 2395.
13. Arıca, M. Y.; Bayramoğlu, G.; Arıca, B.; Yalçın, E.; Ito, K.; Yagci, Y. *Macromol. Biosci.* **2005**, *5*, 983.
14. Gupta, P.; Vermani, K.; Garg, S. *Drug Discov. Today* **2002**, *7*, 569.
15. Ozaydin-Ince, G.; Coclite, A. M.; Gleason, K. K. *Rep. Prog. Phys.* **2012**, *75*, 016501.
16. Asatekin, A.; Barr, M. C.; Baxamusa, S. H.; Lau, K. K. S.; Tenhaeff, W.; Xu, J.; Gleason, K. K. *Mater. Today* **2010**, *13*, 26.
17. Chan, K.; Gleason, K. K. *Langmuir* **2005**, *21*, 8930.
18. Sreenivasan, R.; Bassett, E. K.; Hoganson, D. M.; Vacanti, J. P.; Gleason, K. K. *Biomaterials* **2011**, *32*, 3883.
19. Fineman, M.; Ross, S. D. *J. Polym. Sci.* **1950**, *5*, 259.
20. Lau, K. K. S.; Gleason, K. K. *Macromolecules* **2006**, *39*, 3688.
21. Peppas, N. A.; Barr-Howell, B. D. In Hydrogels in Medicine and Pharmacy, Fundamentals; Peppas, N. A., Ed.; CRC Press: Boca Raton, FL, **1986**; Vol. I, p 27.
22. Baxamusa, S. H.; Montero, L.; Dubach, J. M.; Clark, H. A.; Borros, S.; Gleason, K. K. *Biomacromolecules* **2008**, *9*, 2857.
23. Xu, X.; Goponenko, A. V.; Asher, S. A. *J. Am. Chem. Soc.* **2008**, *130*, 3113.
24. Toomey, R.; Freidank, D.; Rühe, J. *Macromolecules* **2004**, *37*, 882.
25. Mukherjee, M.; Souheib Chebil, M.; Delorme, N.; Gibaud, A. *Polymer* **2013**, *54*, 4669.
26. Peppas, N. A.; Moynihan, H. J.; Lucht, L. M. *J. Biomed. Mater. Res.* **1985**, *19*, 397.
27. Yagüe, J. L.; Gleason, K. K. *Soft Matter* **2012**, *8*, 2890.
28. Bose, R. K.; Lau, K. K. S. *Biomacromolecules* **2010**, *11*, 2116.
29. Asatekin, A.; Gleason, K. K. *Nano Lett.* **2011**, *11*, 677.
30. Wijmans, G.; Baker, R. W. J. *Membr. Sci.* **1995**, *107*(1-2), 1.